THE INFLUENCE OF THE IN-PLANE CONSTRAINT ON THE J RESISTANCE CURVES

A.Neimitz, J.Galkiewicz, R.Molasy

Department of Mechatronics and Machines Design, Kielce University of Technology.
Al. 1000 lecia P.P. 7, 25-314 Kielce, Poland

ABSTRACT

The results of the experimental investigation on the influence of the specimen size and geometry (four specimen configurations) on the J_R curves for two different steels are presented. Side-grooved and non-side-grooved specimens were tested. Two-dimensional finite element modeling (both plane stress and plane strain) of the experimentally tested specimens has been performed. The Q–stresses were determined among other results. The correlations between the trends of the J_R curves and the trends of the $Q=f(a/W)_{J=const}$ or $Q=f(J)_{a/W=const}$ are discussed.

KEYWORDS

J_R curves, Q-stress, stable crack growth, in-plane constraint.

INTRODUCTION

The nature of the stable crack growth is relatively well understood. It is a dissipative process-taking place close to the thermodynamic equilibrium. Thus, the crack growth equation can be considered as the equation representing the sequence of equilibrium states. In principle, this equation can be expressed in a general form:

The crack driving force = The crack growth resistance force

Various quantities were used in the literature as the *crack driving force*. Among them the most popular is the J integral understood as a global quantity not being the path independent or the amplitude of the singular HRR field. Recently, another quantity has been promoted as a good candidate to be utilized in the crack growth equation. It is dissipation rate, R [1] that is considered to have better physical meaning than the J integral. However, it does not solve the basic practical problem, which has been met using both quantities. This problem concerns the quantity called here *the crack growth resistance force.* In both cases it is not a material constant (or better – a material function; since it is a function of the crack extension). It depends not only on the material but on the specimen geometry and size as well as the mode of loading. Numerous experimental and theoretical researches have been undertaken to propose the universal J_R key curves for given materials in order to assure the transferability of results from one to another geometry of the specimen. According to the author's knowledge no full success has been reached so far. The present author and his coworker, following the theoretical analysis [2], proposed the methodology to normalize the J_R curves [3] in order to obtain the transferability of the results. This methodology has been successfully verified experimentally for two materials but only for the one specimen geometry: SENB (single edge notch bending) and for the two extreme cases: the small scale yielding and the fully plastic situation (prior the onset of crack growth). In this method the crack extension Δa was normalized by the length of the ligament

b_0, and the J integral was divided by the quantity proportional to the volume of the plastic zone. For the small scale yielding this quantity was r_p^2, where the r_p is the length of the plastic zone. For the fully plastic case it was the product b_0B, where B is the specimen thickness.

An extensive research has been undertaken to generalize these results to the other specimen configurations and sizes (some of the results of this research are presented in this paper). However, the results obtained were not satisfactory. The main reason for the failure of the methodology proposed is, in our opinion, disability to obtain a closed form formula to compute the volume of the plastic zone for various in- and out-of-plane constraints. Thus, we were not able to compute the quantity, which is necessary to normalize the J integral. The extent of the plastic zone depends on the in- and out-of-plane constraints. The in-plane constraint can be quantified, to some extend, by the Q–stresses [4]. If the Q-stresses, computed prior to the onset of the crack growth, varied according to the similar pattern with changing geometry and sizes of the specimens as the J_R curves it would mean that they could be used to normalize the J_R curves. The appropriate numerical computations have been performed using the ADINA finite element method code. Some of the results obtained are presented in the paper.

THE J_R CURVES – EXPERIMENTAL RESULTS.

The CCT (central crack tension), DNT (double notch tension), SENB (single edge notch bend) and SENT (single edge notched tension) specimens (side-grooved and non side-grooved) were machined and pre-cracked to obtain different in-plane and out-of-plane constraints. More than 120 specimens were tested. They were made of the 40HMNA steel (according to Polish standards, similar to the ASTM 4340 steel) and the 18G2A steel. The chemical composition of both steels and their mechanical properties are shown in Tables 1 and 2. All specimens made of the 40HMNA steel satisfied requirements of the plane strain. Non side-grooved CCT, DNT and SENT specimens made of the 18G2A steel satisfied requirements of the plane stress.

Table.1 Chemical composition

steel	C	Mn	Si	P	S	Cn	V	Cr	Ni	Mo	Cu	Al
18G2A	0.18	1.41	0.38	0.020	0.010	<0.05		<0.05	<0.05	<0.05		<0.025
40HMNA	0.41	0.66	0.25	0.026	0.003		0.01	0.71	1.35	0.20	0.12	

Table.2 Mechanical properties

Steel	σ_0 [MPa]	σ_m [MPa]	A5 [%]	Z [%]
18G2A	383	573	32	68
40 HMNA [N]	1217	1294	9.6	52.6
40HMNA [S]	1173	1247	11.4	53.3
40HMNA [W]	1086	1176	14.1	54.6

The single specimen technique to determine the J_R curves was used. The crack extension was measured using both potential drop and compliance change techniques. The J_R curves for SENB and SENT specimens were determined using the standard formula:

$$J_{i+1} = \left[J_i + \left(\frac{\eta}{b} \right)_i \frac{A_{i,i+1}}{B} \right] \left[1 - \frac{\gamma}{b_i} \left(a_{i+1} - a_i \right) \right] \qquad (1)$$

where $A_{i,i+1}$ is the part of the area under the $P=P(u)$ curve, between the ith and i+1 points along the $P=P(u)$ diagram, u is the load point displacement, B is the specimen thickness, $b=W-a$, W is the width of the specimen, a is the crack length. $\gamma = 1$, $\eta = 2$ for SENB specimens for a/W greater than 0.282. For a/W less than 0.282 η and γ were computed from the formulas known in the literature [5]. From the same source the formulas defining η and γ for SENT specimens were adopted.

For CCT and DNT specimens the following formulas were used:

$$J_i = J_{i-1}\left(1 - \frac{\Delta b}{b_{i-1}}\right) + \frac{1}{Bb_{i-1}}\left(P_{i-1}\Delta u - u_{i-1}\Delta P + \Delta P \Delta u\right), \qquad (2)$$

where

$$J_0 = \frac{1}{Bb_0}\left(2\int_0^{u_0} P_0 du - P_0 u_0\right). \qquad (3)$$

The subscript *0* denotes the point of the crack growth initiation.

Only some of the results obtained for the non side-grooved specimens are presented in this short article. For the side-grooved specimens the J_R curves follow the same pattern as for the non side-grooved specimens however they fall lower than for the non side-grooved specimens. For the CCT and DNT

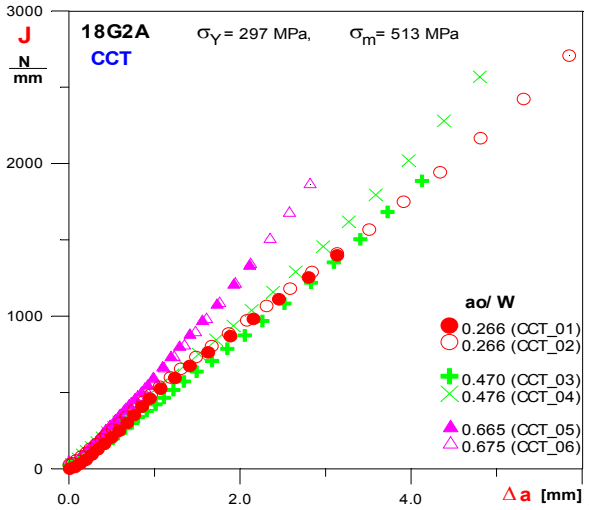

Fig.1a.The J_R curves for the CCT, non – side-grooved specimens made of 18G2A steel. B=3mm.

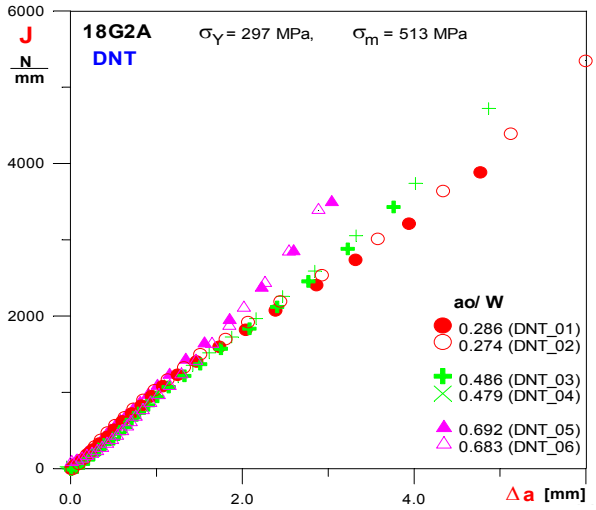

Fig.1b. The J_R curves for the DNT, non-side-grooved specimens made of 18G2A steel. B=3mm.

specimens the longer the initial length of the crack is the higher the J_R curve rise (Figs 1a and 1b). Similar trend was observed for the side-grooved specimens and for the both types of the specimens made of the 40HMNA steel. However, for this steel and both specimens configurations a very short stable crack growth had always been observed before the unstable, cleavage fracture occurred. Different trend was observed for the SENB specimen as shown in Fig.2a. In this case, for both side-grooved and non side-grooved specimens and both steels the J_R curves rise as the crack length decreases. For both types of the SENB specimens and for both steels a long stable crack growth was always observed.

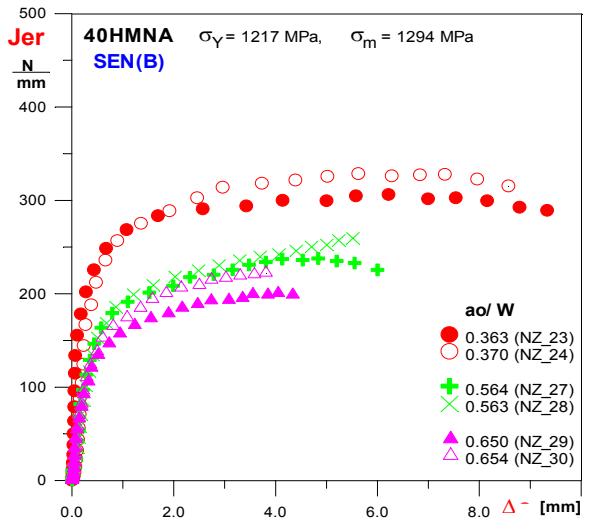

Fig.2a. The J_R curves for the SENB, B=15 mm, 40HMNA steel non-side-grooved specimens

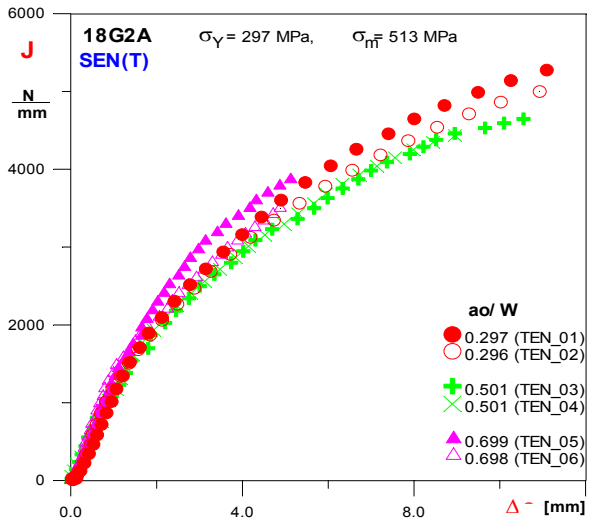

Fig.2b. The J_R curves for the SENT, B=3 mm, 18G2A steel, non-side-grooved specimens

For the SENT specimens the J_R curves run close to each other (Fig.2b) and no particular influence of the initial crack length is observed. It is probably due to the changing mode of loading from the predominantly tensile to bending.

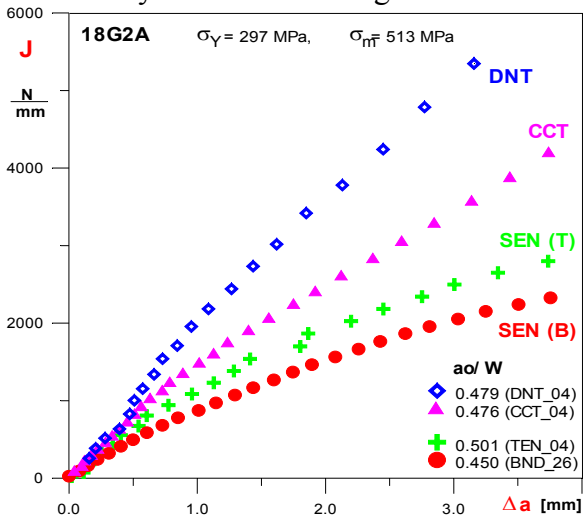

Fig.3. Comparison of the J_R curves for different specimen configurations for the 18G2A steel.

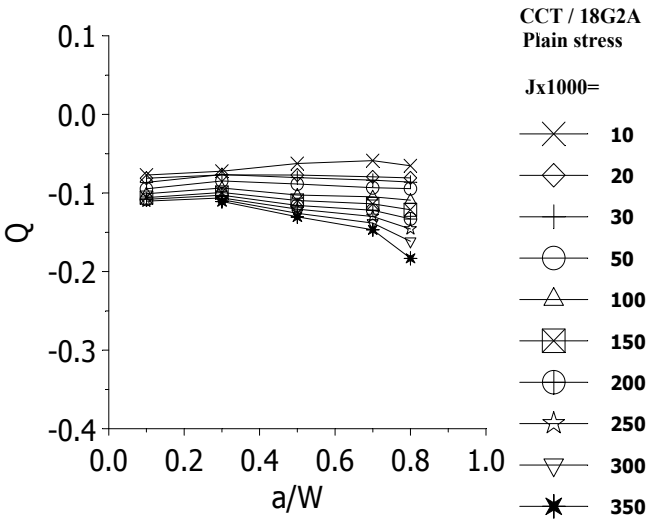

Fig.4. Selected numerical results of the Q-stress computations for the CCT specimens

In Fig.3 the typical trends of the J_R curves for the four specimen configurations are shown. Similar trend was observed for the side-grooved specimens.

NUMERICAL COMPUTATIONS OF THE Q – STRESS.

The finite element computations were carried out with ADINA version 7.4 computer code. All experimentally tested specimens were modeled and computations were made both for the plane strain and plane stress situations for small and finite strains (180 various examples were considered). The finite element meshes were similar to ones used by O'Dowd and Shih [4,6]. Also the methodology to compute the Q–stress followed suggestions of these authors (for the plane stress the similar methodology was used). The Ramberg – Osgood exponents were different for both tested materials. For the 40HMNA steel it was equal to 53 and for the 18G2A steel it was equal to 11. The Q – stresses were computed at the distance $r=2J/\sigma_o$ from the crack tip. In addition to the Q–stresses the stress distributions in front of the cracks were computed as well as the shapes and extents of the plastic zones according to the Huber-Mises-Hencky hypothesis. The results obtained were analyzed along with the experimentally obtained J_R curves. Because of the limited length of this article only few, selected $Q=f(a/W)_{J=const}$ curves are presented for both materials and tested specimens to demonstrate general trends of these curves (Figs 4 and 5). Discussion is included in the next section.

DISCUSSION

In the series of papers by O'Dowd and co-workers (e.g. [4,6]) and other authors the important observations have been made concerning the interrelation between the level of the Q-stress, the extent of plastic deformation and fracture mechanisms. Shortly, the lower the Q-stresses are the less constraint against plastic deformation is observed. With some simplification it may be said that the micro-cracks are generated by high stresses and voids by large strains with a strong shear component. Voids are expected to occur at a high degree of overall (macroscopic) plastic flow, and micro-cracks at a stress build-up without significant relief of plastic flow. In general, both micro-cracks and voids grow inside the grains, thus eventually producing transgranular fracture (Broberg[7]).

One of the aims of the research performed in this project was to compare the behaviour of the J_R curves for various specimen sizes and configurations with the trends of the $Q=f(a/W)_{J=const}$ and $Q=f(J)_{a/W=const}$ functions computed prior to the onset of crack growth for the same specimens. It turns out that many conclusions concerning the stable crack growth can be drown from the shapes of the $Q=f(a/W)_{J=const}$ or $Q=f(J)_{a/W=const}$ curves in accordance with the registered J_R curves and the fractographs. However, it is not so for all types of the specimens tested. Distinct exceptions are the DNT specimens.

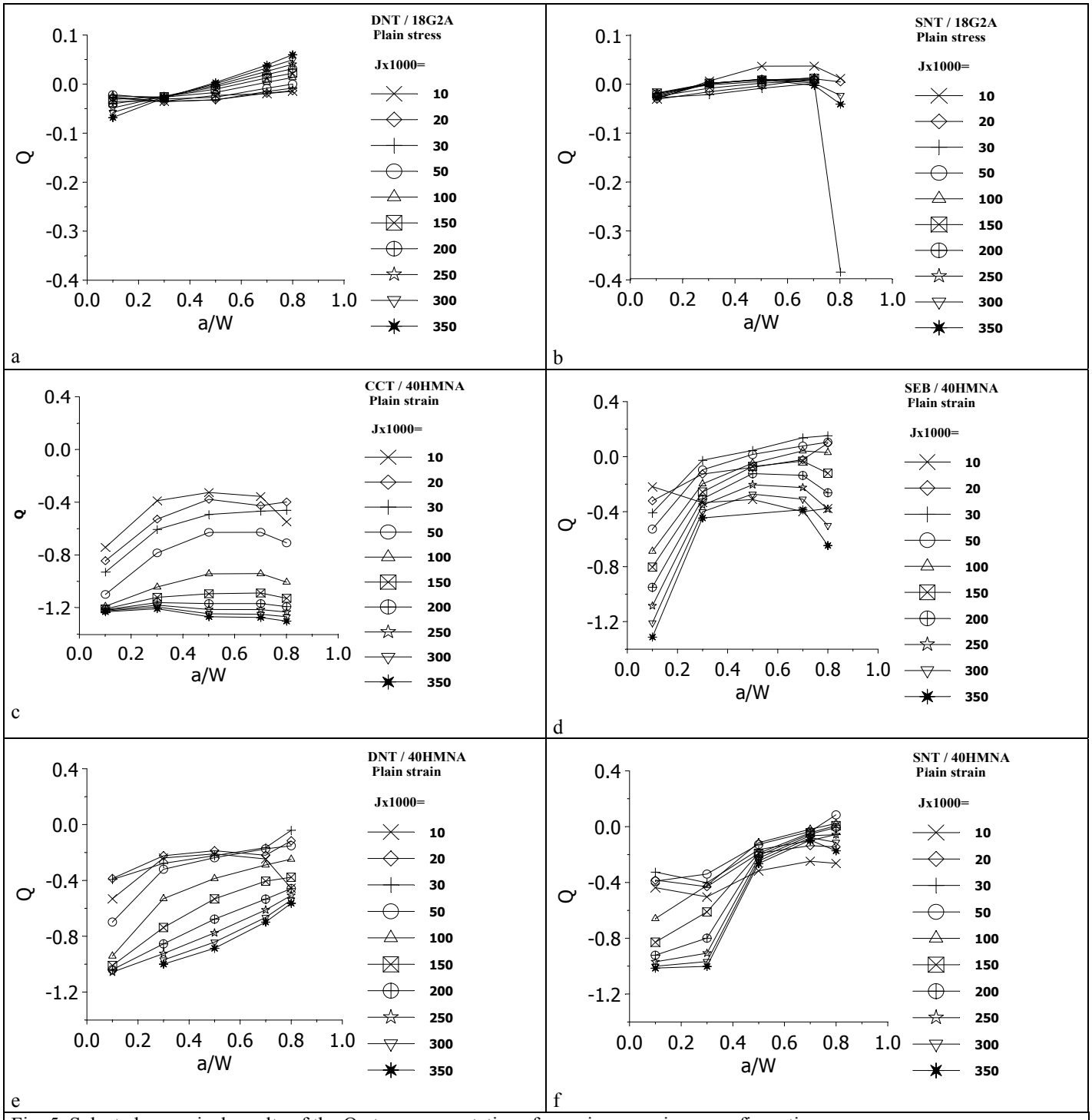

Fig. 5. Selected numerical results of the Q-stress computations for various specimen configurations.

Because of the limited space only few general conclusions can be listed here.

a) For the CCT specimens (plane stress, 18G2A steel, the $J_{IC}\cong 300$ kN/m) the J_R curves rise higher as the initial crack length increases (Fig. 1a). It follows from the numerical computations that the normal stresses as well as the Q-stresses decrease (Fig. 4) in front of the crack when the initial crack length and the J integral increase. Assuming that the similar behaviour may happen for growing cracks, the J_R curves should follow the same pattern as observed experimentally (the smaller Q the less constraint and more dissipation due to the plastic deformation). Sizes of the voids should increase with the crack length. It is also observed experimentally (because of the limited volume of the paper the fractographs are not shown here). The J_R curves for the side-grooved specimens followed the same pattern although they run lower than for the non-side-grooved specimens. The normal stress components for side-grooved specimens are higher than for the plane stress situation. Moreover, the plastic deformation is more

localized because of the stronger geometrical constraints. Plastic dissipation is less for these specimens thus, the J_R curves run lower than for the non-side-grooved specimens.

b) For the SENT specimens (plane stress) the Q stresses are close to zero (Fig. 5b) and they do not change much with the initial crack length. One could conclude that the J_R curves should not be much dependent on the a_o/W. Indeed, we observed such a trend of the J_R curves for this specimen configuration (Fig.2b). The J_R curves for the SENT specimens (plane stress) should run below the curves for the CCT specimens since the normal stresses and the Q-stresses in front of the crack are higher for the former specimens. This behaviour was also observed experimentally (Fig.3).

c) For all types of the specimens considered the lowest J_R curves are for the SENB specimens (Fig.3). It also can be predicted from the analysis of the normal stress components in front of the crack. However, in this case the results for the plane strain (SENB specimen) and plane stress (other specimen shapes) must be compared.

d) For the SENB specimens J_R curves follow different pattern than for the CCT specimens. For the shortest crack the J_R curves rise highest (Fig.2a). This phenomenon can also be explained through the analysis of the normal stresses or the Q-stresses in front of the crack. For the SENB specimen geometry the Q-stress increases with the a_o/W.

Above observations would suggest that the Q-stress could have been considered a proper parameter to be used to normalize the J integral along ordinate in order to assure transferability of the J_R curves. However, the numerical results obtained for the DNT specimens lead to the conclusions which are in the total conflict with experimental observations. For the DNT specimens (plane stress, 18G2A steel) the Q-stresses are negative and close to zero (Fig.5a) for small a_o/W and increase for greater a_o/W reaching positive values. The Q-stresses for the DNT specimens are greater than for CCT and SENT ones. Thus, one could expect that the J_R curves for the DNT specimens should run below the J_R curves for the CCT and SENT specimens. In fact it is inversely (Fig. 3).

Since the Q-stresses increase with a_o/W (for the DNT specimens) one could expect that the J_R curves should follow the pattern similar to the SENB specimens (the highest curves for the shortest crack). It is again inversely. However, the sizes of the voids, observed in the fractographs, decrease with increasing a_o/W and this is the only observation, which agrees with the theoretical prediction (the greater Q the smaller void diameter). The only qualitative explanation, so far, of this exceptional (among tested specimen configurations) behaviour of the DNT specimens follows from the analysis of the shapes and sizes of the plastic zones in front of the crack. Detailed numerical analysis of this problem has been performed. For the material tested (18G2A steel, plane stress) and for the loading close to the critical one the plastic zone grows bigger than for the CCT and SENT specimens and it is not limited to the well defined shapes and sizes following from the size and shape of the specimens. Thus, one could conclude that the Q-stress alone is not able to give the full information on the loss of the in-plane constraint for all geometrical shapes of the specimen.

Acknowledgements

Authors gratefully acknowledge support from the Polish National Research Committee, grant No.7 T07C 008 15

REFERENCES

1. Turner, C.E. (1990) In: *Fracture Behaviour and Design of Materials and Structures, 8th European Conference on Fracture* (ed. D.Firrao), Vol.II, EMAS, Warley, UK,pp.933-968.
2. Neimitz, A., (1996). In: *Constitutive Relation in High/very High Strain Rates*, (ed. K.Kawata and J.Shiori), Springer-Verlag, Tokyo, pp. 92-104
3. Neimitz, A. Molasy, R. (1998),.In: *Fracture from Defects, 12th European Conference on Fracture* (ed. M.W.Brown, E.R. de los Rios and K.J.Miller), EMAS, pp. 787-812,
4. O'Dowd, N.P., Shih, C.F. , (1991), *J.Mech. Phys. Solids,* Vol.39, No.8, str. 989-1015,
5. Link, R.E. and Joyce, J.A.,(1996), *Application of Fracture Toughness Scalling Models to the Ductile-to-Brittle Transition,* NUREG/CR-6279, U.S.Nuclear Regulatory Commission, NRC Job Code J6036, Washington
6. O'Dowd, N..P., (1995), *Engineering Fracture Mechanics* Vol.52, No.3, str. 445-465.
7. Broberg, K.B., (1999), *„Crack and Fracture",* Academic Press